J Appl Physiol 109: 1675–1685, 2010.
First published October 14, 2010; doi:10.1152/japplphysiol.01372.2009.

The Na^+/Ca^{2+} exchanger-1 mediates left ventricular dysfunction in mice with chronic intermittent hypoxia

Ling Chen,[1,2] Jin Zhang,[2] Xuejiao Hu,[3] Kenneth D. Philipson,[4] and Steven M. Scharf[1]

Departments of [1]Medicine and [2]Physiology, University of Maryland, Baltimore, Baltimore, Maryland; [3]Department of Pathology, Womack Army Medical Center, Ft. Bragg, North Carolina; and [4]Department of Physiology, David Geffen School of Medicine at University of California Los Angeles, Los Angeles, California

Submitted 9 December 2009; accepted in final form 29 September 2010

Chen L, Zhang J, Hu X, Philipson KD, Scharf SM. The Na^+/Ca^{2+} exchanger-1 mediates left ventricular dysfunction in mice with chronic intermittent hypoxia. *J Appl Physiol* 109: 1675–1685, 2010. First published October 14, 2010; doi:10.1152/japplphysiol.01372.2009.—Chronic intermittent hypoxia (CIH) and cardiovascular dysfunction occur in patients with obstructive sleep apnea. We hypothesized that the Na^+/Ca^{2+} exchanger-1 (NCX1) mediates, at least partially, left ventricular (LV) dysfunction in CIH. Four groups of mice (N = 15–17 per group), either cardiac-specific NCX1 knockouts (KO) or wild types (WT), were exposed to either CIH or normoxia [i.e., handled controls (HC)] 10 h/day for 8 wk. As expected, myocardial expression of NCX1 was greater in WT than in KO animals, both in HC and CIH-exposed groups. In both CIH groups (WT or KO), but not the HC groups, blood pressure increased by 10% at *week 1* over their baseline and remained elevated for all 8 wk, with no differences between WT and KO. LV dilation (increased diastolic and systolic dimension) and hypertrophy (increased left heart weight), along with LV dysfunction (greater end-diastolic pressure and lower ejection fraction), were observed in the WT animals compared with the KO following CIH exposure. Compared with HC, CIH exposure was associated with apoptosis (terminal deoxynucleotidyl transferase dUTP-mediated nick-end labeling and caspase-3) in WT, but not KO, mice. We conclude that myocardial NCX1 does not mediate changes in blood pressure, but is one of the mediators for LV global dysfunction and cardiomyocyte injury in CIH.

sleep apnea; hypertension; hypertrophy; heart failure; apoptosis

OBSTRUCTIVE SLEEP APNEA (OSA) is a common disease, affecting 2–4% of the general population (36), with even higher prevalence among the elderly and the overweight. Population-based studies suggest that OSA is an independent risk factor for several cardiovascular diseases, such as hypertension, coronary artery disease, congestive heart failure, and stroke (1, 19, 32). The mechanisms responsible for this link are still unclear; however, repetitive upper airway obstruction can lead to chronic intermittent hypoxia (CIH), exaggerated swings in intrathoracic pressure, and postapneic arousals, with resultant abnormalities in neural, humoral, vascular, inflammatory, and metabolic pathways (32).

In rats, CIH leads to several of the cardiovascular consequences seen in human OSA, including blood pressure (BP) elevation, biventricular hypertrophy, and left ventricular (LV) contractile dysfunction (5, 6, 9, 33, 35). These were shown to be associated with increased LV myocardial apoptosis and oxidative stress (5, 6, 35). Recent studies in mice observed similar changes in BP following CIH exposure (4, 22). Because of the availability of genetically engineered mouse lines, the mouse model provides a potentially powerful tool for studying the molecular mechanisms responsible for cardiovascular damage in CIH.

The Na^+/Ca^{2+} exchanger isoform-1 (NCX1) is a membrane transporter ubiquitously expressed in all cell types and organs. It is the dominant isoform in the myocardium and mediates the electrogenic countertransport of three Na^+ ions for one Ca^{2+} ion across the sarcolemmal membrane. This process is bidirectional and can produce either Ca^{2+} efflux (i.e., forward mode) from or influx (i.e., reverse mode) to cells (29). The forward mode activity is the dominant mechanism behind the extrusion of intracellular Ca^{2+}; thus it plays a pivotal role in Ca^{2+} homeostasis for electrical-contraction coupling on a beat-to-beat basis (2). The reverse-mode activity may also be a physiological mechanism leading to Ca^{2+} entry into the cytoplasm, as in the case of Ca^{2+}-induced Ca^{2+} release from the sarcoplasmic reticulum (SR) during the early phase of cardiac contraction (31). However, elevated reverse-mode activity results in abnormal Ca^{2+} homeostasis and electrical activity, which is considered as an important pathway leading to cardiac injury (34).

A mouse line with specific ablation of cardiac NCX1 (KO) has been created (12), and these animals are, as expected, more resistant to ischemia-reperfusion (I/R) injury than wild-type (WT) controls (13). CIH results in periodic hypoxia and reoxygenation that may be reminiscent of I/R. Thus NCX1 may be a mediator of cardiovascular damage during CIH. We used the CIH model in mice to test the following hypotheses: *1*) CIH leads to BP elevation and LV dysfunction in WT mice; and *2*) cardiac-specific ablation of NCX1 protects hearts from dysfunction in CIH.

MATERIALS AND METHODS

Animals and Intermittent Hypoxia Exposure

The protocols for this study were approved by the Institutional Animal Care and Use Committee of University of Maryland. Mice with cardiac-specific ablation of NCX1 (KO) were previously created with a genetic background of C57BL/6 (12). The present study used only male adults, either KO or WT littermates, age 6–7 mo. Mice were assigned into four groups in total (N = 15–17 for each group), with KO and their siblings from the same cage, and were exposed to either CIH or normoxia [similarly handled controls (HC)]. Thus the four groups were as follows: KO/HC (KO mice exposed to HC), KO/CIH (KO mice exposed to CIH), WT/HC (WT mice exposed to HC), and WT/CIH (WT mice exposed to CIH). Those who performed the data collection or calculations were blinded to the treatment groups, which included measurement of tail-cuff BP and apoptosis, calculations from echocardiographic images and cardiac catheterization, and evaluations of LV histology.

Address for reprint requests and other correspondence: L. Chen, 685 W. Baltimore St., MSTF 816, Baltimore, MD 21201 (e-mail: Lchen@medicine.umaryland.edu).

The protocol for the CIH or HC exposure previously reported in rats (5, 6, 35) was used here with only minor modifications. In brief, the animals were housed in the Central Animal Facility with a light-dark cycle of 12:12 h and were given free access to food and water. The animals were then placed in the chambers of an environment system (HypOxyc system, Kent Scientific, Torrington, CT) for the exposure, with free mobility and access to water and food. The oxygen concentration of each chamber was monitored and controlled by a computer via servo-operated solenoids introducing either N_2 or room air into the chambers. For CIH exposure, nitrogen was flushed into the chamber for ~40 s. Once a nadir O_2 concentration of 4–5% was reached, normoxia was produced by flushing in room air (21% O_2), leading rapidly back to chamber O_2 concentration of 21%. This cycle was repeated for 10 h/day, 7 days/wk during the daylight hours over 8 wk. When not in the exposure chambers, animals were returned to their home cages in the housing facility. HC animals were handled similarly to the CIH-exposed animals. They were placed in similar chambers on the same bench top, for the same periods of time as CIH, but were exposed only to a continuous flow of room air.

Systolic BP. Systolic BP (SBP) was measured with the animals conscious and restrained, using a tail-cuff system (Hatteras Instruments, model MC4000, Cary, NC) at baseline (e.g., before the first exposure) and the end of *weeks 1*, *2*, *4*, and *8*. The same animals were used for echocardiography and cardiac catheterization, as described below. For measurements of SBP, animals were restrained in a mouse holder integrated with a heating pad set to 95°F. To minimize measurement variation, animals were acclimatized to the restraint system for 5–10 min for 2 consecutive days before the baseline measurements. The tail cuff was inflated and deflated for 5 initial cycles for further acclimatization, followed by 10 averaged measurements to produce the final result. In pilot studies before these, the tail-cuff system was validated by simultaneous recordings of SBP via the tail-cuff system and an intra-arterial catheter (1.4 French, Millar Instruments, Houston, TX) inserted into the right carotid artery under general anesthesia with isoflurane. The correlation coefficient (r^2) for the linear regression was 0.96 (unpublished data), indicating excellent agreement between the two methods.

Echocardiography. Echocardiography was performed under anesthesia (inhalation of 1.2–1.5% isoflurane in oxygen), at baseline and at the end of 8 wk. A core temperature of 37.5°C was maintained during the measurement. Transthoracic M-mode images of the LV in the parasternal short-axis view were obtained at the level of the papillary muscles using high-resolution ultrasound biomicroscopy equipped with a 40-MHz scanhead (Vevo 770, VisualSonics, Toronto, Canada). The indexes directly measured include heart rate, LV cavitary dimensions in diastole (LVDd) and systole (LVDs), and LV posterior wall thickness in diastole and systole. LV fractional shortening was calculated as [(LVDd − LVDs)/LVDd] × 100. LV end-diastolic volume was calculated as {[7/(2.4 + LVDd)] × $LVDd^3$}, and LV end-systolic volume as {[7/(2.4 + LVDs)] × $LVDs^3$}. LV ejection fraction (EF) was calculated as [(LV end-diastolic volume − LV end-systolic volume)/LV end-diastolic volume] × 100.

Cardiac catheterization. Cardiac catheterization was performed at the end of 8 wk under anesthesia with 1.5–2% isoflurane. Two micromanometer-tipped catheters (Millar Instruments, Houston, TX) were inserted into the LV and the superior vena cava, from the right carotid artery and the right jugular vein, respectively. Once the catheters were positioned, isoflurane was reduced to 1.2%, followed by recordings of LV pressure and central venous pressure onto a computer-based data system (BioPac Systems, Goleta, CA). The LV catheter was then pulled back to the ascending aorta for BP measurement. Both catheters were then removed and replaced with a 1-Fr thermocouple (Columbia Instruments, Columbus, OH) into the ascending aorta and PE-10 tubing into the right atrium. Cardiac output (CO) was measured at least three times using thermodilution technique (Cardiomax III, Columbia Instruments), with a bolus injection of 50 μl cold (4°C) physiological saline into the right atrium. The indexes calculated included the following: mean BP (MBP), LV end-diastolic pressure (LVEDP), maximal first time derivative of LV pressure rise (dP/dt_{max}), and systemic vascular resistance (SVR) [SVR = (MBP − mean central venous pressure)/CO].

Animals were euthanized by cervical dislocation following cardiac catheterization. The hearts were rapidly excised and perfused with a cold physiological saline. The heart specimens were weighed and used for in vitro analyses.

Real-time Polymerase Chain Reaction and Western Blot

Using previously described methods (5, 6), we measured the mRNA expression of NCX1, β-myosin heavy chain (β-MHC), atrial natriuretic peptide (ANP), and 18s rRNA (a "housekeeping gene"). In brief, the LV free wall was homogenized in a Trizol reagent (Invitrogen, Burlington, ON, Canada). RNA was recovered from the aqueous phase following centrifugation. First-strand cDNA was synthesized using the Superscript-II system (Invitrogen). Real-time polymerase chain reaction was performed in 20-μl reaction volumes using SYBRgreen JumpStart *Taq* ReadyMix DNA polymerase (Sigma-Aldrich). Fluorescence was measured with a DNA Engine Opticon 2 system (MJ Research, Waltham, MA). Polymerase chain reaction conditions and cycle number were optimized accordingly for each set of the primers of NCX1, ANP, β-MHC, and 18s rRNA. We normalized all mRNA levels to the level of 18s rRNA.

For the Western blot, the total protein was isolated from the LV tissue by homogenization and lysis with a complete protease inhibitor (Roche Diagnostics, Indianapolis, IN). Protein concentration was measured using a Bradford protein assay kit (Bio-Rad, Hercules, CA). Thirty micrograms of protein were loaded into a 10% SDS-polyacrylamide gel electrophoresis and then transferred into a nylon membrane (Amersham Biosciences, Piscataway, NJ). The NCX1 and β-actin antibodies were obtained from Chemicon International (catalog no. AB3516P, Temecula, CA). The blots were developed using chemiluminescence (NEN Life Science, Boston, MA) and quantified by densitometry (Alpha Innotech, San Leandro, CA). NCX1 results are presented as a ratio to β-actin.

Heart histology. As previously described (6), hearts were cut into 5-μm slices following 10% formalin fixation and paraffin embedding. The sections were then deparaffinized, rehydrated, and stained with Masson-trichrome by standard methods. Digital images of the LV free wall were obtained using a Zeiss microscope equipped with Axio Vision software (Carl Zeiss Imaging Solutions). The images were used for the measurement of cardiomyocyte cross-sectional area and fibrosis area using ImageJ software (http://rsbweb.nih.gov/ij/). At least 100 randomly selected cardiomyocytes per heart were measured and averaged over the cell number. The fibrosis area was measured over more than 20 randomly selected square of field (1 mm^2) per heart and is presented as a percentage of total area.

Apoptosis. Apoptosis was assessed by terminal deoxynucleotidyl transferase-mediated dUTP nick end labeling (TUNEL) and caspase-3 activity assay. The TUNEL staining and methyl green counterstaining were performed using TdT-FragEL apoptosis detection kits (Calbiochem, San Diego, CA), according to the manufacturer's instructions. TUNEL-positive nuclei in the LV free wall were counted within a 4-mm^2 square of field. The number was averaged over four randomly selected fields per section and five sections per heart. Caspase-3 activity was measured using a commercially available assay kit (Calbiochem), per the manufacturer's instruction. In brief, LV free wall tissues were freshly collected and homogenized at 4°C. Ten microliters of the extract were mixed with 40 μl of the assay buffer and then reacted with 50 μl of the caspase-3 substrate containing 200 μM of Ac-DEVD-pNA. The absorbance was measured at 405 nM at 5-min intervals for 120 min. Triplicate measurements of each homogenate were averaged and then normalized by protein concentration measured via Bradford protein assay kit.

Statistics

Statistical analysis was performed using GB-stat V9 (Dynamic Microsystems, Silver Spring, MD). All of the data showed a normal distribution, as determined by the Kolmogorov-Smirnov test. Data were presented as means ± SE. For data collected only at *week 8*, statistical significance was tested using two-factor ANOVA: one factor being genotype (WT or KO), and one factor being exposure treatment (HC or CIH). For data collected over time, including body weight, tail BP, and echocardiographic variables, three-factor ANOVA was performed, with the additional factor being time. To reduce variability between animals at baseline, the echocardiographic data were additionally analyzed as the changes at *week 8* compared with baseline (i.e., delta) and then tested by two-factor ANOVA. If significance was found, the source of significance was determined after adjusting for multiple comparisons using post hoc Newman-Keuls analysis. We explored the interaction between the two primary factors, genotype (WT or KO) and exposure (HC or CIH). Interaction represents the degree to which differences between levels of one factor are influenced by the level of the other. The null hypothesis was rejected at the 5% level.

RESULTS

BP

There were no significant differences in tail SBP (Fig. 1*A*) between groups at baseline or over time for either HC group (KO or WT). However, SBP increased over time in both CIH groups at *week 1*, and remained elevated at *weeks 2*, *4*, and *8*, compared with their own baseline ($P < 0.05$, respectively). There were no differences between genotypes with either CIH or HC at any time point. At the end of *week 8*, MBP measured via intra-arterial catheter (Fig. 1*B*) was elevated in both CIH groups (WT and KO) compared with HC and with no significant differences between genotypes for either HC or CIH exposure. Thus CIH was associated with increased BP, an effect not mitigated by changes in genotype.

Body Weight

Body weight (Table 1) increased at *week 8* over baseline for HC animals for both genotypes, but not in the two groups exposed to CIH. The differences between the genotypes were not significant.

Echocardiographic Data

As Table 1 shows, there were no significant differences in any indexes between the groups at baseline. Comparing *week 8* to baseline (Table 1), the WT with CIH, but not the KO with CIH, had significantly higher LVDd and LVDs, which suggests ventricular remodeling; higher LV posterior wall thickness in diastole, indicating LV hypertrophy; and lower LV fractional shortening and LVEF, indicating contractile dysfunction. In the case of LVDs and LVEF, the difference at *week 8* between WT and KO animals exposed to CIH also reached significance after adjustment for multiple comparisons ($P < 0.01$ or 0.05, respectively). The other echocardiographic variables did not show significance when comparing WT and KO animals at *week 8* following CIH exposure. These findings are further strengthened by the significant difference in change (Δ) in LVDd, ΔLVDs, and ΔLVEF between the two CIH groups (Fig. 2). Thus, in the KO animals, compared with WT, the effects of exposure to CIH on LV dimension and function (LVEF) appeared to be mitigated. As shown in Table 1, none of the interactions between genotype and exposure were significant in this analysis. In Fig. 2, the interaction terms for LVDd and LVDs between genotype and exposure did reach statistical significance.

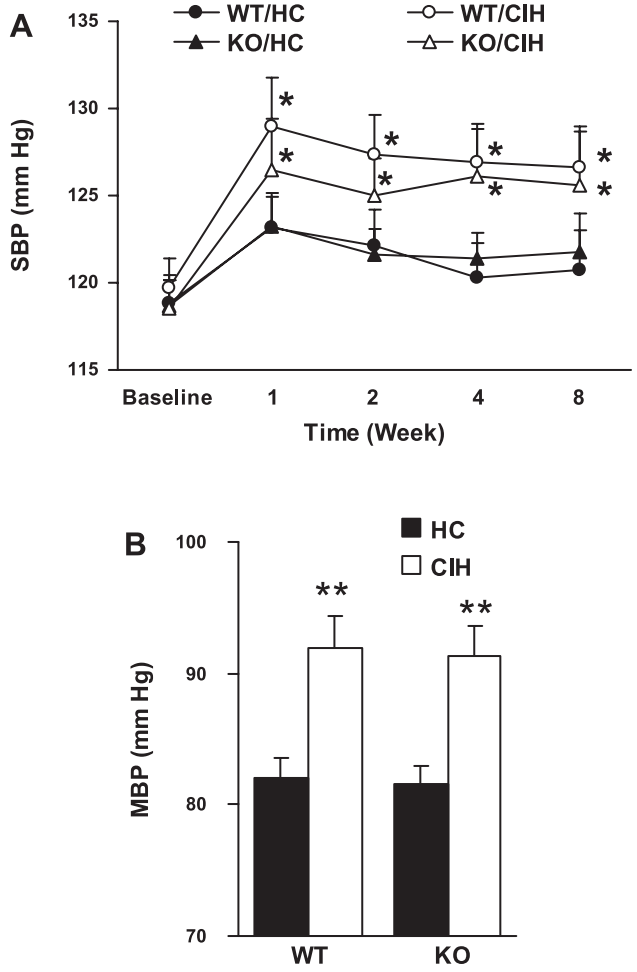

Fig. 1. *A*: systolic blood pressure (SBP) measured by the tail cuff over time ($n = 15$ each group). WT/HC, wild type with handled control; WT/CIH, wild type with chronic intermittent hypoxic exposure; KO/HC, cardiac-specific Na^+/Ca^{2+} exchanger isoform-1 (NCX1) knockout with handled controls; KO/CIH, cardiac-specific NCX1 knockout with chronic intermittent hypoxic exposure. *$P < 0.05$ compared with their own baseline. *B*: mean BP (MBP) measured by intra-arterial catheter at *week 8* ($n = 15$–17). **$P < 0.01$, compared with either WT/HC or KO/HC. Values are means ± SE.

Cardiac Catheterization

There were no effects of CIH or genotype on heart rate (WT/HC: 411 ± 13.9; WT/CIH: 428 ± 13.3; KO/HC: 424 ± 8.6; KO/CIH: 422 ± 13.4 beats/min; $P > 0.05$). In the WT animals, compared with the HC mice, CIH exposure was associated with increased LVEDP (Fig. 3*A*) and SVR (*B*), and decreased CO (*C*) and dP/dt_{max} (*D*). However, in the KO animals, there were no significant differences in any of these variables between HC and CIH. For LVEDP, the differences between the WT and the KO groups with CIH exposure were significant. However, for CO and dP/dt_{max}, the differences between genotypes with CIH did not reach statistical significance. For SVR, CO, and dP/dt_{max}, differences between WT/

Table 1. *Body weight and echocardiographic data*

					P			
	WT/HC	WT/CIH	KO/HC	KO/CIH	WT/HC vs. WT/CIH	KO/HC vs. KO/CIH	WT/HC vs. KO/HC	WT/CIH vs. KO/CIH
BW, g								
Base	36.7 ± 0.6	37.8 ± 0.6	36.8 ± 0.6	37.4 ± 0.6	NS	NS	NS	NS
Week 8	40.8 ± 0.6	38.0 ± 0.8	39.9 ± 0.6	38.0 ± 0.7	<0.05	NS	NS	NS
P (base vs. *week 8*)	<0.01	NS	<0.01	NS		Interaction, genotype vs. exposure: NS		
LVDd, mm								
Base	2.76 ± 0.11	2.71 ± 0.09	2.81 ± 0.10	2.84 ± 0.10	NS	NS	NS	NS
Week 8	2.96 ± 0.10	3.34 ± 0.18	3.01 ± 0.08	3.05 ± 0.14	<0.05	NS	NS	NS
P (base vs. *week 8*)	NS	<0.01	NS	NS		Interaction, genotype vs. exposure: NS		
LVDs, mm								
Base	1.59 ± 0.05	1.60 ± 0.05	1.64 ± 0.05	1.67 ± 0.08	NS	NS	NS	NS
Week 8	1.70 ± 0.08	2.13 ± 0.14	1.76 ± 0.05	1.84 ± 0.09	<0.01	NS	NS	<0.01
P (base vs. *week 8*)	NS	<0.01	NS	NS		Interaction, genotype vs. exposure: NS		
LVPWd, mm								
Base	1.19 ± 0.05	1.27 ± 0.03	1.23 ± 0.09	1.26 ± 0.07	NS	NS	NS	NS
Week 8	1.30 ± 0.08	1.57 ± 0.06	1.27 ± 0.11	1.47 ± 0.08	<0.05	NS	NS	NS
P (base vs. *week 8*)	NS	<0.01	NS	<.05		Interaction, genotype vs. exposure: NS		
LVFS, %								
Base	41.8 ± 1.5	40.7 ± 1.3	41.4 ± 1.2	41.0 ± 1.2	NS	NS	NS	NS
Week 8	42.9 ± 1.4	36.1 ± 1.7	41.4 ± 1.2	39.6 ± 1.3	<0.05	NS	NS	NS
P (base vs. *week 8*)	NS	<0.05	NS	NS		Interaction, genotype vs. exposure: NS		
LVEF, %								
Base	74.1 ± 1.7	73.1 ± 1.3	73.8 ± 1.3	73.3 ± 1.3	NS	NS	NS	NS
Week 8	75.2 ± 1.7	66.5 ± 2.3	73.5 ± 1.4	71.4 ± 1.6	<0.055	NS	NS	<0.05
P (base vs. *week 8*)	NS	<0.05	NS	NS		Interaction, genotype vs. exposure: NS		

Values are means ± SE; $N = 15$–17 for each group. WT, wild type; HC, handled controls; CIH, chronic intermittent hypoxia; KO, knockout; BW, body weight; NS, not significant. Groups are as follows: WT/HC (WT mice exposed to HC), WT/CIH (WT mice exposed to CIH), KO/HC (KO mice exposed to HC), and KO/CIH (KO mice exposed to CIH). Echocardiographic parameters include the following: LVDd, left ventricular diastolic dimension; LVDs, left ventricular systolic dimension; LVPWd, left ventricular posterior wall diastolic thickness; LVFS, left ventricular fractional shortening; LVEF, left ventricular ejection fraction. Three-factor ANOVA was used for variables measured at baseline and 8 wk, and two-factor ANOVA for variables measured only at *week 8*.

CIH and KO/CIH were not significant. Statistical significance was not reached for the interactions between genotype and exposure for any of the variables measured at catheterization.

Heart Weights

Total heart (HW) and left heart weights (LHW), and the ratio of both weights to body weight, were higher at 8 wk in the WT animals exposed to CIH compared with HC (Fig. 4). However, in the KO animals, none of the weights was higher with CIH exposure compared with the HC animals. Furthermore, with CIH exposure, these weights and their ratios to body weight were greater in the WT animals compared with the KO animals. Thus KO appeared to mitigate effects of CIH on HW and LHW. However, statistical significance was not reached for the interactions between genotype and exposure for any of the HW-related variables.

Myocardial mRNA and Protein Expression

As expected, in the KO animals with HC, myocardial expression of NCX1 mRNA (Fig. 5*A*) and protein (*B* and *C*) were substantially reduced compared with the WT with HC. For the WT animals, compared with the HC, CIH was associated with increased expression of both mRNA and protein. On the other hand, for the KO genotype, there was no significant difference in NCX1 expression between CIH and HC. Myocardial mRNA expression of β-MHC (Fig. 5*D*) and ANP (*E*) were similar at HC groups with the WT and KO genotypes. However, expression of these two heart failure genes was higher in the CIH vs. the HC animals for the WT, but not for the KO genotype. The differences between WT/CIH and KO/CIH for β-MHC and ANP were not significant. The interactions between genotype and exposure were significant for NCX1 mRNA and NCX1 protein.

Heart Histology and Apoptosis Assays

For the WT animals, myocyte cross-sectional area was ~12% higher in CIH compared with HC ($P < 0.05$) (Fig. 6). For the KO animals, the difference between HC and CIH did not reach significance. There was no significant difference in fibrosis area with CIH compared with HC for either genotype. In the WT animals, compared with the HC animals, CIH was associated with greater TUNEL positivity and caspase-3 activity. However, for the KO animals, there was no significant difference between CIH and HC. None of the differences between WT/CIH and KO/CIH were significant. Moreover, statistical significance was not reached for the interactions between genotype and exposure for any of the histological variables.

DISCUSSION

There are two major findings in this study. First, CIH exposure was associated with sustained elevations in BP over the course of the exposure. This was observed in both NCX1 KO and WT mice, suggesting that the cardiac NCX1 did little to mediate the BP changes. Second, following CIH exposure, compared with WT animals, KO animals showed significantly less myocardial dilation (LVDd and LVDs) and hypertrophy (HW and LHW), improved systolic function (LVEF), and lower LVEDP. These findings paralleled elevations of LV apoptosis and protein and/or mRNA expression of NCX1,

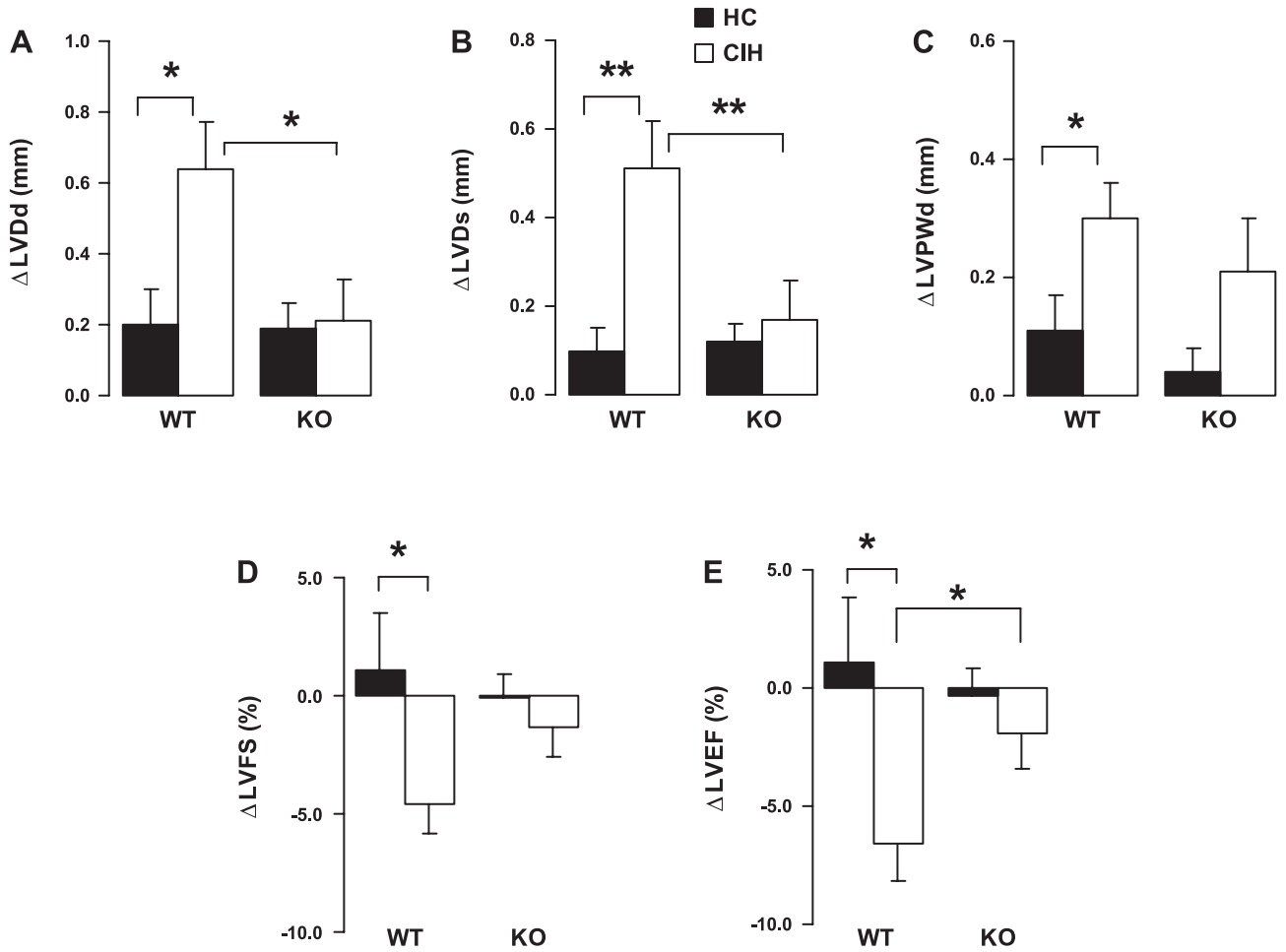

Fig. 2. Changes (Δ) in echocardiographic indexes at *week 8* over baseline. Values are means ± SE; $N = 15$ each group. *A* and *B*: changes of left ventricular (LV) diastolic (ΔLVDd; *A*) and systolic (ΔLVDs; *B*) dimension at *week 8* over baseline. *C*: changes of LV posterior wall diastolic thickness (ΔLVPWd) at *week 8* over baseline. *D*: changes of LV fractional shortening (ΔLVFS). *E*: changes of LV ejection fraction (ΔLVEF) at *week 8* over baseline. $*P < 0.05$; $**P < 0.01$. Significance of interaction between genotype (WT or KO) and exposure (HC or CIH): for LVDd, $P < 0.05$; for LVDs, $P = 0.0074$; nonsignificant (NS) for LVPWd, LVFS, and LVEF.

β-MHC, and ANP seen in WT, but not KO, animals following CIH exposure compared with HC. Hence, our data strongly suggest that NCX1 plays an important role as a pathway to cardiac dysfunction and damage in CIH. In the ensuing discussion, we consider these findings in the light of the limitations of the experimental model and currently available literature.

Cardiovascular Dysfunction in CIH

Humans with sleep apnea develop both CIH and cardiovascular dysfunction. Animal models of CIH mimic several cardiovascular features in OSA, supporting CIH as a cause or important contributor in development of cardiovascular dysfunction. Indeed, our results show BP increases of ~10% in WT with CIH, compared with baseline or HC (Fig. 1). These findings are consistent with the previously reported findings in rats by several groups, including ours (5, 6, 9, 33, 35), and in mice by others (4). The proposed mechanisms for the BP changes include the activation of sympathoadrenal activity (9, 28) and increases in vascular reactivity (17, 29, 33). While BP elevations may contribute somewhat to myocardial hypertrophy, both changes are not closely coupled in CIH models, with a greater severity in hypertrophy (5, 6). In the present study, despite similar BP changes in both CIH groups (see below), myocardial dysfunction was found only in the HC. The separation of BP and myocardial changes provides direct evidence suggesting that the mechanisms leading to hypertension are different from those leading to myocardial dysfunction in this model.

As our laboratory reported previously (5, 6, 35), LV dysfunction develops in rats exposed to CIH and includes hypertrophy, remodeling, contractile dysfunction, myocardial apoptosis, oxidative stress, and elevated expression of several hypertrophy "marker" genes. In C57BL/6 mice exposed to CIH, Campen et al. (4) reported an increased HW-to-body weight ratio, a consequence of body weight loss, rather than of an increase in HW. In the present study, body weight (Table 1) was lower in both CIH groups at *week 8* compared with the HC groups, but not compared with baseline; thus there was no loss of body weight in our studies. The body weight changes in the CIH groups are associated with the CIH exposure, but not to the status of cardiac function, since the KO animals with CIH had no sign of cardiac dysfunction (see below). In the present study, LV hypertrophy was evident in WT mice following

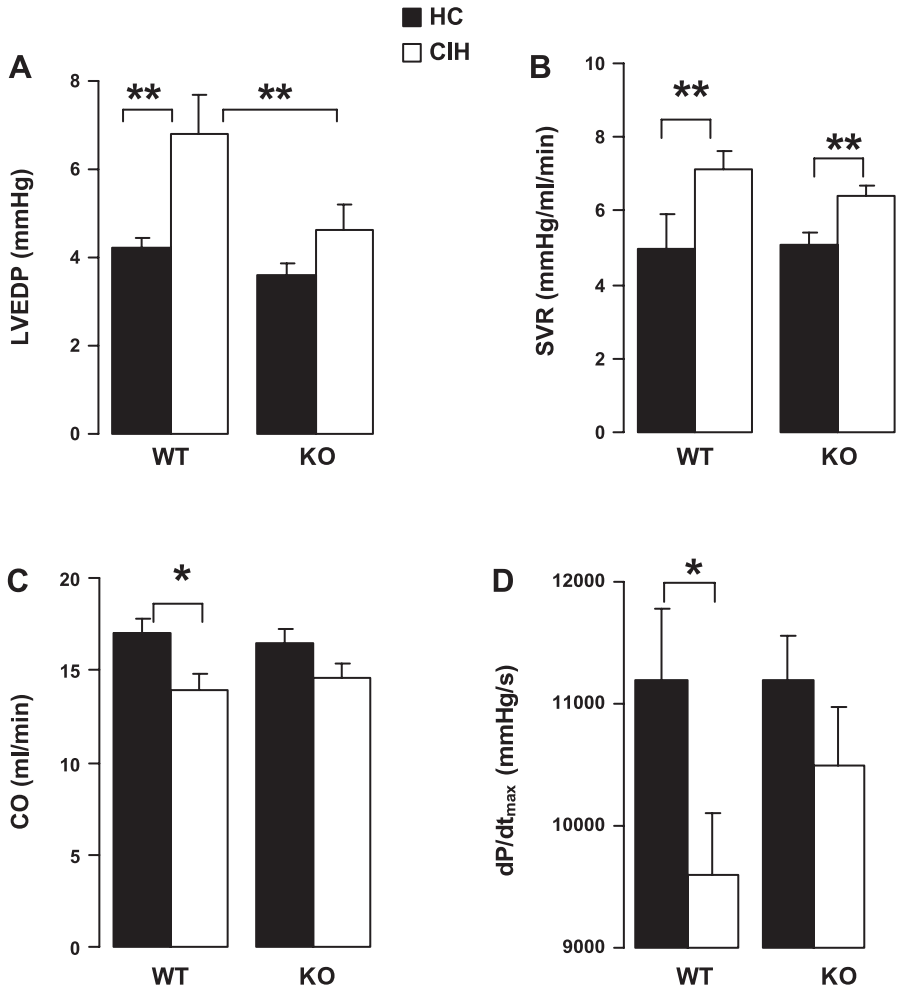

Fig. 3. Indexes of LV function measured by cardiac catheterization at *week 8*. Values are means ± SE; $N = 16$ for WT/HC, 17 for WT/CIH, and 15 for others. *A*: LV end-diastolic pressure (LVEDP). *B*: systemic vascular resistance (SVR). *C*: cardiac output (CO). *D*: the first derivatives of LV pressure rise (dP/dt_{max}). $^*P < 0.05$; $^{**}P < 0.01$. Significance of interaction between genotype (WT or KO) and exposure (HC or CIH): NS for SVR, LVEDP, CO, and dP/dt_{max}.

8-wk exposure to CIH, indicated by three lines of evidence: increases in LHW with or without normalization to body weight (Fig. 4), increases in LV posterior wall thickness via echocardiography (Table 1 and Fig. 2), and increases in cardiomyocyte cross-sectional area via histology (Fig. 6). Furthermore, the WT animals showed LV remodeling with CIH at *week 8*, indicated by increases in LVDs and LVDd (Table 1 and Fig. 2) compared with their baseline. None of these changes was observed in the KO mice. Furthermore, the differences at *week 8* of CIH exposure were significant and indicated worsening LV function and remodeling in the WT compared with KO animals. Similarly, systolic dysfunction also developed in WT/CIH, suggested by the measures of echocardiography (Table 1 and Fig. 2) and catheterization (Fig. 3) variables, changes not seen in the KO animals. By direct comparison following CIH exposure, LV dilation (LVDd and LVDs) and systolic dysfunction (LVEF) were clearly worse in the KO, but not the WT, animals.

Our findings on LV dysfunction with CIH are consistent with our laboratory's previous observations in rats (5, 6, 35). However, a recent report by Naghshin et al. (22) in mice observed increased LV contractility, findings different than those reported here. Since the C57BL/6 strain was used in the Naghshin study, as well as ours, the genetic background of the animals is unlikely to be responsible for the different findings. The exact cause for the discrepancy between our study and that of Naghshin et al. is unclear; however, there were differences in animal age and exposure protocol used in the two studies. While the present study used mice at 24–28 wk, with an exposure of 8 wk, the Naghshin study used younger mice at age of 9–10 wk, with a shorter exposure lasting 4 wk. OSA is a chronic disease, with higher prevalence in older individuals (1, 19, 32); thus the present protocol is possibly more relevant for the human condition. On the other hand, the present study required the animals to be transferred daily between the housing and exposure facilities. It remains possible that animals exposed to CIH might have developed a conditioned fear to the hypoxia chamber that contributed to cardiac dysfunction. Finally, the difference in animal age between the present study and in the previous studies by others (4, 22), and the fact that the mice were fed ad libitum likely account for the finding that the mice in our group were heavier than previously reported.

We examined several cellular changes that may underlie LV global dysfunction in animals exposed to CIH. Cardiomyocyte cross-sectional area increased with CIH exposure in WT, but not KO, animals (Fig. 6*A*), suggesting that hypertrophy occurs at the cardiomyocyte level following CIH. Hypertrophy is one of the major responses of cardiomyocytes to mechanical and neurohormonal stress. As suggested by numerous studies, hypertrophy may initially represent an adaptive response, but ultimately is responsible for ventricular dilatation and heart failure, which is one of the leading causes of mortality and

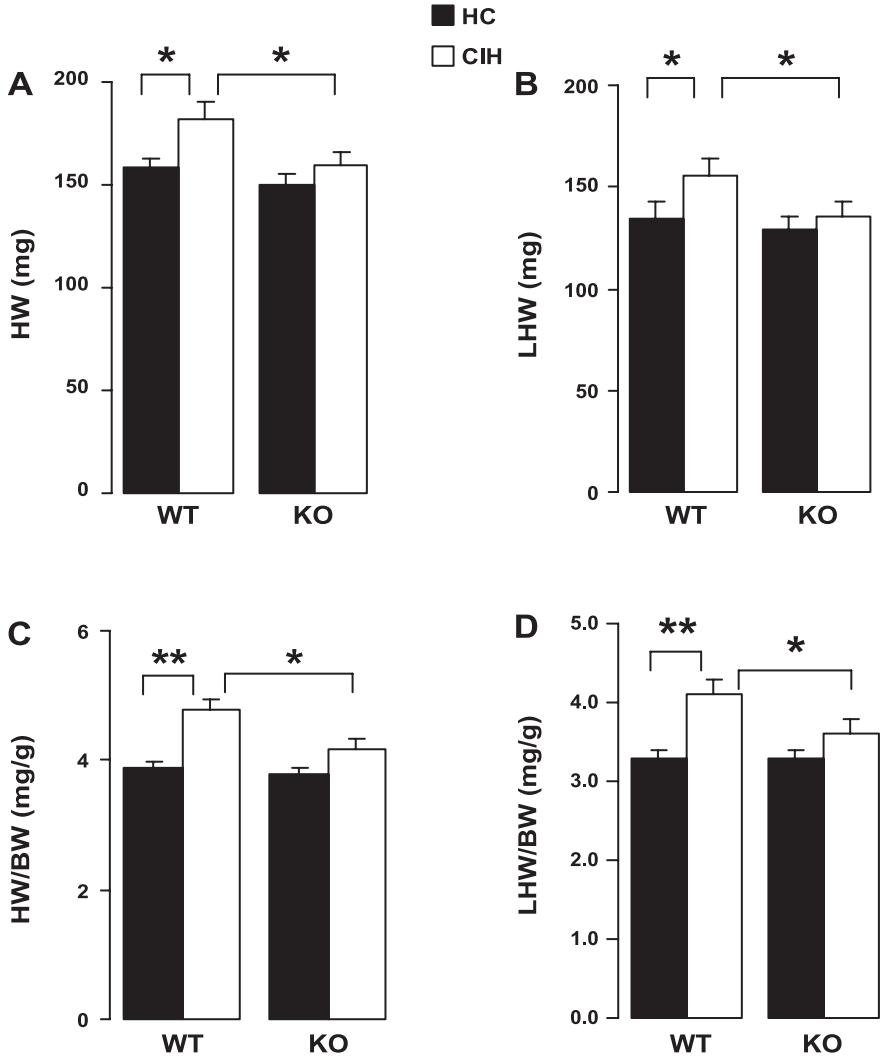

Fig. 4. Total heart weight (HW; *A*), left heart (equals left free wall plus intraventricular septal) weight (LHW; *B*), and their ratios to body weight (BW; *C* and *D*, respectively). Values are means ± SE; $N = 15$ each group. $^{*}P < 0.05$; $^{**}P < 0.01$. Significance of interaction between genotype and exposure: NS for HW, LHW, LWH/BW, and HW/BW.

morbidity. Moreover, with CIH, WT mice showed increased myocardial apoptosis (Fig. 6). Apoptosis is known to contribute to the deterioration of ventricular function in certain cardiac pathologies (7). It could well be that the decline in myocardial function following 8-wk exposure to CIH relates, at least in part, to cellular drop-out from apoptosis. LV expression of β-MHC and ANP mRNA, the genes usually upregulated in myocardial hypertrophy, was elevated in the WT mice with CIH (Fig. 5). Finally, consistent with our previous study in rats, we found no evidence for increased myocardial fibrosis with CIH, although myocardial fibrosis usually occurs in experimental and human heart failure. We did not observe significant changes in myocardial cross-sectional area, or indexes of apoptosis (TUNEL and caspase-3) in the KO animals with CIH compared with HC, but did observe this in the WT animals. We believe that these findings indicate some mitigation of this response to CIH with the KO mice. However, on direct comparison, the differences between WT and KO animals with CIH exposure did not reach statistical significance. This may be attributed to variability in the measurements, along with the relatively small numbers involved.

Myocardial NCX1 in CIH

In the present study, myocardial expression of NCX1 mRNA and protein doubled in the WT animals with CIH compared with the WT with HC, while the differences between both KO groups were insignificant (Fig. 5). In human and experimental cardiovascular diseases, the myocardial expression of NCX1 was elevated and was closely associated with cardiac dysfunction (3, 11, 14, 25, 30), suggesting an important role of NCX1 in the cardiac pathogenesis. The mechanism for the NCX1 upregulation observed in CIH is unclear. Sympathetic activation is common in OSA patients (19, 32), as well as in the rat model of CIH (9, 33). β-Adrenergic stimulation has been shown to upregulate NCX1 at the transcriptional and protein levels (10, 21). Furthermore, NCX1 mediates the anti-remodeling effects of the β-blocker metoprolol (20). On the other hand, chronic ganglionic blockade eliminated hypertension but not LV hypertrophy (9), suggesting that sympathetic stimulation plays a limited role in myocardial changes. At the posttranscriptional level, NCX1 activity and its forward or reverse mode are dependent on the transmembrane electrochemical gradient, especially on intracellular Na^+ concentra-

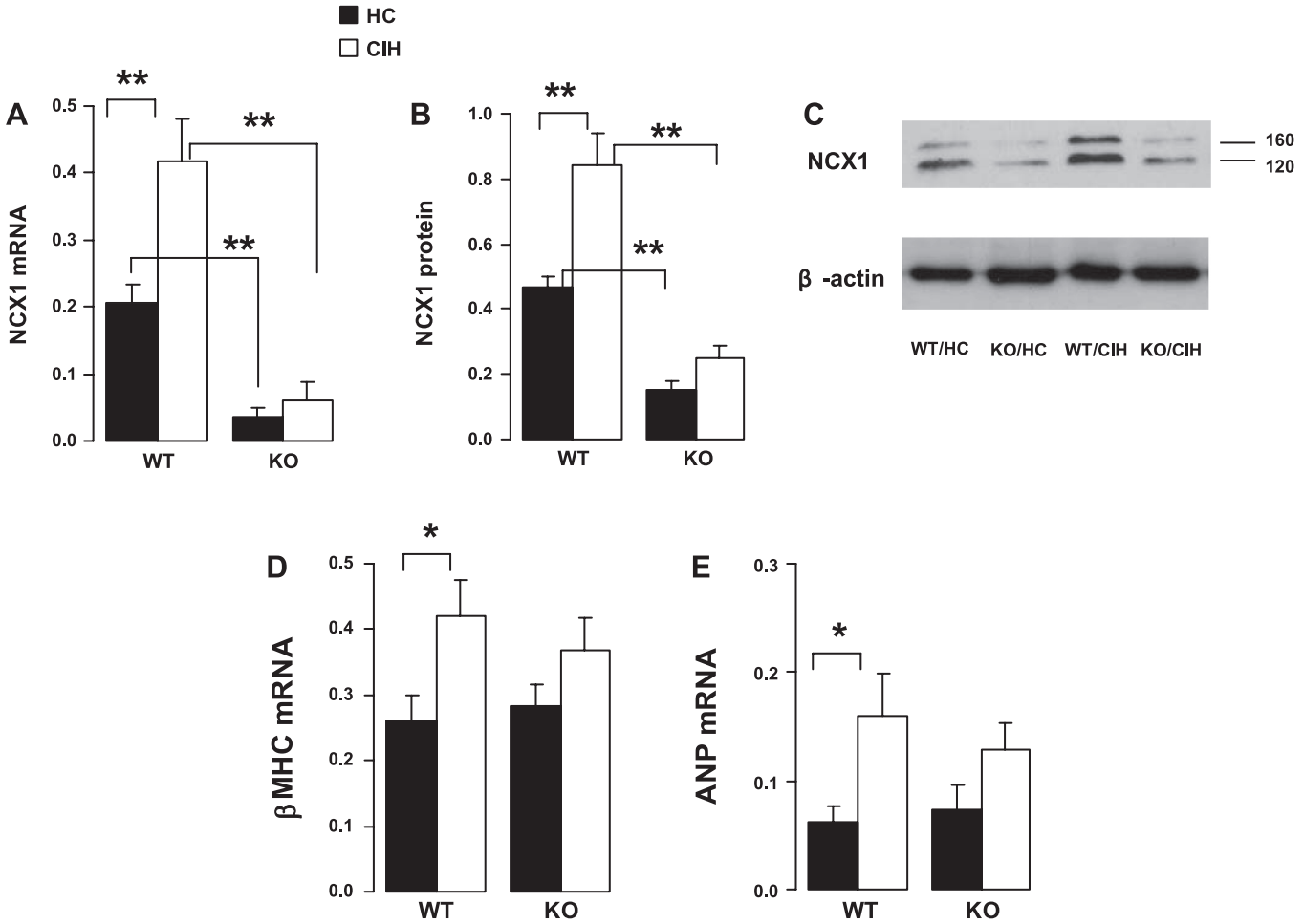

Fig. 5. Gene and protein expression of selected genes in the LV myocardium. *A*: myocardial expression of NCX1 mRNA as ratio of 18s rRNA. *B*: myocardial expression of NCX1 protein as ratio of β-actin. *C*: representative results of Western blot for NCX1 (*top*) and β-actin (*bottom*) from one animal from each group. The 120-kb band was used for quantification of NCX1 expression presented in *B*. *D* and *E*: myocardial expression of β-myosin heavy chain (MHC) and atrial natriuretic peptide (ANP) as ratio of 18s rRNA, respectively. Values are means ± SE; $N = 6$ each group. *$P < 0.01$; **$P < 0.01$. Significance for interaction between genotype and exposure: for NCX mRNA, $P = 0.02$; for NCX protein, $P = 0.02$; NS for β-MHC and ANP.

tion, which is normally controlled by Na^+-K^+-ATPase (Na^+ pump). In I/R, Na^+ pump activity is inhibited because of decreases in ATP production, which reduces Na^+ efflux via the pumps. In other hands, increases in H^+ production would facilitate Na^+ influx via Na^+/H^+ exchanger-1. Both effects lead to Na^+ concentration overload (24) that facilitates reverse-mode activity of NCX1. This mechanism may also occur in the myocardium with CIH. Finally, oxidative stress is considered to be an important contributor to cardiovascular injury in OSA (18), a contention supported by findings in rats exposed to CIH (5, 35). Therefore, oxidative stress may also modulate NCX1 activity. Consistent with this notion are recent findings of redox-mediated regulation of NCX1 activity in vitro (8, 16).

The KO mice used in this study were created by targeting and deleting *exon 11* from the NCX1 gene, which ablated the exchanger from 80–90% of the cardiomyocytes (12). In the present study, the KO/HC mice expressed ~10% of NCX1 mRNA, but 35% of the NCX1 protein in the myocardium, as that in the WT/HC animals (Fig. 5). Residual NCX1 activity in KO mice has been noted previously (12). The explanation in the cited study was that the cardiac-specific KOs do not occur with 100% efficiency. Cells in which excision occurs will have a complete absence of NCX1, and the remaining cells will have a normal expression level. In addition, there is also the possibility that, in some cells, the excision occurs on only one allele, leaving some residual activity.

We note, however, that Henderson et al. (12) showed a 20–30% reduction in LV function with NCX KO compared with WT. By contrast, in the present study, we did not find changes in any of the variables, except for NCX1 expression, including LV function measured echocardiographically or by catheterization in the KO group not exposed to CIH (HC group). The reasons for the discrepant results are not clear. However, we observed greater residual expression of NCX1 protein in the KO mice, and the mice used in the present were considerably older (6–7 mo) than those in the Henderson et al. study (7–8 wk). It is possible that, in our study, the greater baseline NCX1 expression mitigated decreases in LV function with the KO, or that, with increasing age, other Ca^{2+} transport mechanisms are activated.

How could NCX1 KO myocytes survive, considering the key role played by NCX1 in Ca^{2+} efflux following each excitation? Previous studies have suggested alternative efflux

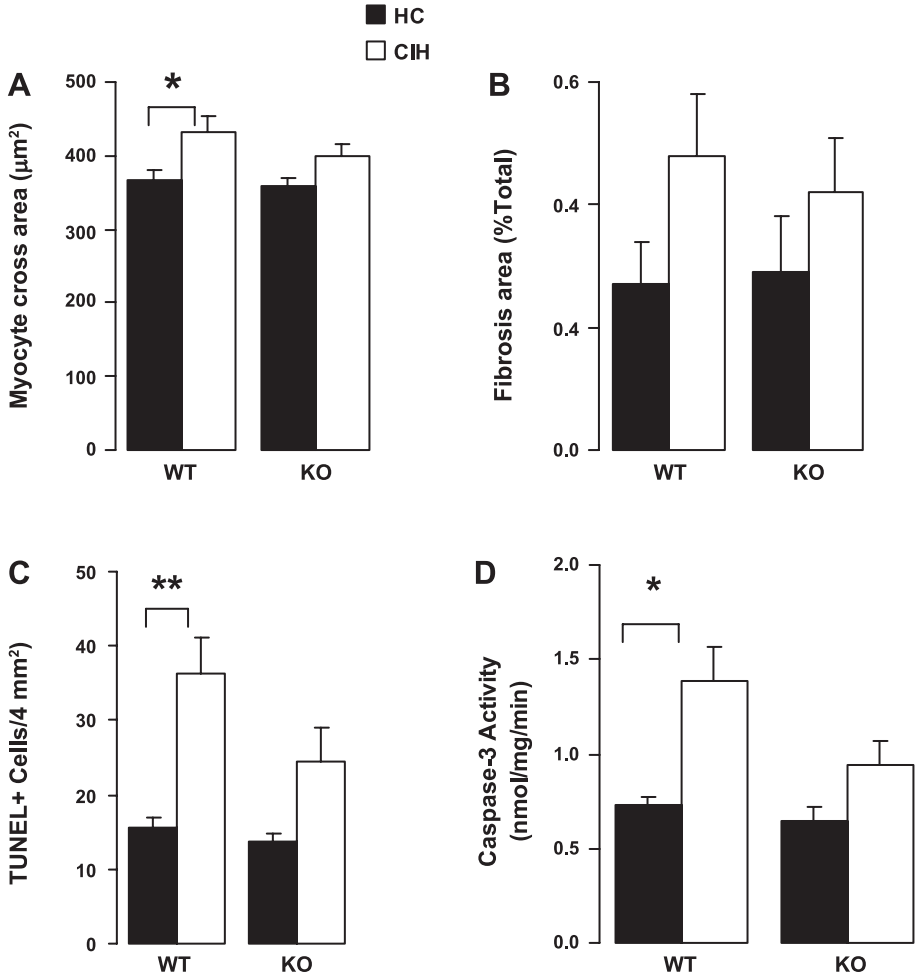

Fig. 6. Heart histology and apoptosis assays. *A* and *B*: LV cardiomyocyte cross area (μm^2) and fibrosis area (%total area), respectively, were measured in Mason trichrome-stained heart slices. Values are means ± SE; $N = 6$ each group. *C*: terminal deoxynucleotidyl transferase-mediated dUTP nick end labeling (TUNEL)-positive cell number per 4 mm^2 in TUNEL-stained LV free wall tissues. *D*: caspase-3 activity in the LV myocardial homogenates. *C* and *D*, $N = 7$ for WT/CIH, and 8 for other groups. $^*P < 0.05$; $^{**}P < 0.01$. Significance of interaction between genotype and exposure: NS for cardiomyocyte cross area, fibrosis area, TUNEL positive cell number, and caspase-3 activity.

mechanisms developed in the KO myocytes, including decreases in Ca^{2+} influx via L-type Ca^{2+} channels, increases of plasma membrane Ca^{2+} ATPase activity in posttranscriptional level, and increases in Ca^{2+} release from SR (12, 26, 27).

One of the major findings in the present study is the beneficial effects of cardiac NCX1 KO in CIH. This is indicated by the lack of effect of indexes of LV global and cellular dysfunction discussed above following CIH exposure in KO as opposed to WT mice. As noted, at *week 8* following CIH exposure, there were a number of significant differences between KO and WT animals, such that indexes of LV function were worse in the WT animals. A number of other indexes were noted to change for the worse in the WT, but not KO, animals, although direct comparisons following CIH did not reach significance. Specifically, the NCX KO mice did not show the same degree of change in LVDd and LVDs and LV contractile function (LVEF and LVEDP), and LHW and total HW seen with the WT mice following CIH exposure. Taken as a whole, our findings indicate that cardiac NCX1 mediates, at least in part, the LV dysfunction in CIH. Our results are also consistent with a previous study (13) that showed that the hearts from the NCX1 KO mouse line were more resistant to I/R in vitro.

We cannot say with certainty how the reduction of NCX1 protects the heart in CIH. One possibility is the "excessive" reverse (Ca^{2+} influx) mode of NCX1 activity, which has long been thought to be the principle pathway of Ca^{2+} overload in cardiac pathologies, such as I/R-induced hypertrophy and heart failure (34). The disturbance in Ca^{2+} homeostasis, including the elevation of cytosolic Ca^{2+} concentration and abnormal SR release, then disrupts normal functions of cardiac cells, with impaired electrical activity and contractile dysfunction (34). Indeed, NCX1 inhibitors, KB-R7943, and SEA0400, showed reduced Ca^{2+} influx and improved ventricular function in a failing heart (34). Moreover, Na^+/H^+ exchanger-1 inhibitors are cardioprotective in several animal models, based on the inhibition of Na^+-dependent Ca^{2+} overload via the reverse-mode NCX1 (15).

We note that, in some cases, the interaction term did not appear to support conclusions based on the pairwise analysis adjusted for multiple comparisons. This likely reflects the small sample sizes and variable measures of the data. The fact that interactions were significant for mRNA and protein expression of NCX1 and changes in LV cavitary dimensions measured by echocardiography are additional strong support for our thesis that NCX1 mediates many of the changes occurring with CIH exposure.

Finally, although we studied the myocardial NCX1 in the present study, extramyocardial NCX1 in CIH may also contribute to cardiovascular responses to CIH. Indeed, smooth muscle NCX1 appears important in BP regulation in rodents. For example, our recent study showed that specific KO of

smooth muscle NCX1 lowered mouse BP in vivo and attenuated vasoconstriction in isolated mesenteric artery (37). Consistently, smooth muscle NCX1 upregulated in the Milan hypertensive rats, which is likely responsible for the BP changes through a pathway related to transient receptor potential canonical 6 and Ca^{2+} signaling (38).

In conclusion, as in the rat model, C57BL/6 mice developed BP elevation and LV dysfunction with exposure to CIH. The ablation of cardiac NCX1 attenuates LV dysfunction following CIH, but has no effects on the BP changes. Therefore, myocardial NCX1 is one of the major molecular mediators of LV dysfunction in CIH. BP elevation in CIH does not play a major role in development of LV dysfunction.

ACKNOWLEDGMENTS

Juan Wu provided technical support.

GRANTS

This study was supported by a grant-in-aid from the Mid-Atlantic American Heart Association (0765262U, L. Chen). S. M. Scharf was supported by National Heart, Lung, and Blood Institute Grant HL074441.

DISCLOSURES

No conflicts of interest, financial or otherwise, are declared by the author(s).

REFERENCES

1. **Ancoli-Israel S, DuHamel ER, Stepnowsky C, Engler R, Cohen-Zion M, Marler M.** The relationship between congestive heart failure, sleep apnea, and mortality in older men. *Chest* 24: 1400–1405, 2003.
2. **Bers DM.** Cardiac excitation-contraction coupling. *Nature* 415: 198–205, 2002.
3. **Brooks WW, Bing OH, Boluyt MO, Malhotra A, Morgan JP, Satoh N, Colucci WS, Conrad CH.** Altered inotropic responsiveness and gene expression of hypertrophied myocardium with captopril. *Hypertension* 35: 1203–1209, 2000.
4. **Campen MJ, Shimoda LA, O'Donnell CP.** Acute and chronic cardiovascular effects of intermittent hypoxia in C57BL/6J mice. *J Appl Physiol* 99: 2028–2035, 2005.
5. **Chen L, Einbinder E, Zhang Q, Hasday J, Balke CW, Scharf SM.** Oxidative stress and left ventricular function with chronic intermittent hypoxia in rats. *Am J Respir Crit Care Med* 172: 915–920, 2005.
6. **Chen L, Zhang J, Gan TX, Chen-Izu Y, Hasday JD, Karmazyn M, Balke CW, Scharf SM.** Left ventricular dysfunction and associated cellular injury in rats exposed to chronic intermittent hypoxia. *J Appl Physiol* 104: 218–223, 2008.
7. **Diez J, Gonzalez A, Lopez B, Querejeta R.** Mechanisms of disease: pathologic structural remodeling is more than adaptive hypertrophy in hypertensive heart disease. *Nat Clin Pract Cardiovasc Med* 2: 209–216, 2005.
8. **Eigel BN, Gursahani H, Hadley RW.** ROS are required for rapid reactivation of Na^+/Ca^{2+} exchanger in hypoxic reoxygenated guinea pig ventricular myocytes. *Am J Physiol Heart Circ Physiol* 286: H955–H963, 2004.
9. **Fletcher EC.** Invited review: Physiological consequences of intermittent hypoxia: systemic blood pressure. *J Appl Physiol* 90: 1600–1605, 2001.
10. **Golden KL, Fan QI, Chen B, Ren J, O'Connor J, Marsh JD.** Adrenergic stimulation regulates Na^+/Ca^{2+} exchanger expression in rat cardiac myocytes. *J Mol Cell Cardiol* 32: 611–620, 2000.
11. **Hasenfuss G, Schillinger W, Lehnart SE, Preuss M, Pieske B, Maier LS, Prestle J, Minami K, Just H.** Relationship between Na^+-Ca^{2+}-exchanger protein levels and diastolic function of failing human myocardium. *Circulation* 99: 641–648, 1999.
12. **Henderson SA, Goldhaber JI, So JM, Han T, Motter C, Ngo A, Chantawansri C, Ritter MR, Friedlander M, Nicoll DA, Frank JS, Jordan MC, Roos KP, Ross RS, Philipson KD.** Functional adult myocardium in the absence of Na^+-Ca^{2+} exchange: cardiac-specific knockout of NCX1. *Circ Res* 95: 604–611, 2004.
13. **Imahashi K, Pott C, Goldhaber JI, Steenbergen C, Philipson KD, Murphy E.** Cardiac-specific ablation of the Na^+-Ca^{2+} exchanger confers protection against ischemia/reperfusion injury. *Circ Res* 97: 916–921, 2005.
14. **Ito K, Yan X, Tajima M, Su Z, Barry WH, Lorell BH.** Contractile reserve and intracellular calcium regulation in mouse myocytes from normal and hypertrophied failing hearts. *Circ Res* 87: 588–595, 2000.
15. **Karmazyn M, Kilić A, Javadov S.** The role of NHE-1 in myocardial hypertrophy and remodelling. *J Mol Cell Cardiol* 44: 647–653, 2008.
16. **Kuster GM, Lancel S, Zhang J, Communal C, Trucillo MP, Lim CC, Pfister O, Weinberg EO, Cohen RA, Liao R, Siwik DA, Colucci WS.** Redox-mediated reciprocal regulation of SERCA and Na^+-Ca^{2+} exchanger contributes to sarcoplasmic reticulum Ca^{2+} depletion in cardiac myocytes. *Free Radic Biol Med* 48: 1182–1187, 2010.
17. **Lefebvre B, Godin-Ribuot D, Joyeux-Faure M, Caron F, Bessard G, Lévy P, Stanke-Labesque F.** Functional assessment of vascular reactivity after chronic intermittent hypoxia in the rat. *Respir Physiol Neurobiol* 150: 278–286, 2006.
18. **Lavie L, Lavie P.** Molecular mechanisms of cardiovascular disease in OSAHS: the oxidative stress link. *Eur Respir J* 33: 1467–1484, 2009.
19. **Leung RS, Bradley TD.** Sleep apnea and cardiovascular disease. *Am J Respir Crit Care Med* 164: 2147–2165, 2001.
20. **Maczewski M, Mackiewicz U.** Effect of metoprolol and ivabradine on left ventricular remodelling and Ca^{2+} handling in the post-infarction rat heart. *Cardiovasc Res* 79: 42–51, 2008.
21. **Mani SK, Egan EA, Addy BK, Grimm M, Kasiganesan H, Thiyagarajan T, Renaud L, Brown JH, Kern CB, Menick DR.** β-Adrenergic receptor stimulated Ncx1 upregulation is mediated via a CaMKII/AP-1 signaling pathway in adult cardiomyocytes. *J Mol Cell Cardiol* 48: 342–351, 2010.
22. **Naghshin J, McGaffin KR, Witham WG, Mathier MA, Romano LC, Smith SH, Janczewski AM, Kirk JA, Shroff SG, O'Donnell CP.** Chronic intermittent hypoxia increases left ventricular contractility in C57BL/6J mice. *J Appl Physiol* 107: 787–793, 2009.
23. **Phillips SA, Olson EB, Lombard JH, Morgan BJ.** Chronic intermittent hypoxia alters NE reactivity and mechanics of skeletal muscle resistance arteries. *J Appl Physiol* 100: 1117–1123, 2006.
24. **Pieske B, Houser SR.** $[Na^+]_i$ handling in the failing human heart. *Cardiovasc Res* 57: 874–886, 2003.
25. **Pogwizd SM, Schlotthauer K, Li L, Yuan W, Bers DM.** Arrhythmogenesis and contractile dysfunction in heart failure: Roles of sodium-calcium exchange, inward rectifier potassium current, and residual beta-adrenergic responsiveness. *Circ Res* 88: 1159–1167, 2001.
26. **Pott C, Henderson SA, Goldhaber JI, Philipson KD.** Na^+/Ca^{2+} exchanger knockout mice: plasticity of cardiac excitation-contraction coupling. *Ann N Y Acad Sci* 1099: 270–275, 2007.
27. **Pott C, Philpson KD, Goldhaber JI.** Excitation-contraction coupling in Na^+-Ca^{2+} exchanger knockout mice: reduced transarcolemmal Ca^{2+} flux. *Circ Res* 97: 1288–1295, 2005.
28. **Prabhakar NR, Dick TE, Nanduri J, Kumar GK.** Systemic, cellular and molecular analysis of chemoreflex-mediated sympathoexcitation by chronic intermittent hypoxia. *Exp Physiol* 92: 39–44, 2007.
29. **Quednau BD, Nicoll DA, Philipson KD.** The sodium/calcium exchanger family-SLC8. *Pflügers Arch* 447: 543–548, 2004.
30. **Ranu HK, Terracciano CM, Davia K, Bernobich E, Chaudhri B, Robinson SE, Bin Kang Z, Hajjar RJ, MacLeod KT, Harding SE.** Effects of Na^+/Ca^{2+}-exchanger overexpression on excitation-contraction coupling in adult rabbit ventricular myocytes. *J Mol Cell Cardiol* 34: 389–400, 2002.
31. **Sipido KR, Maes M, Van de Werf F.** Low efficiency of Ca^{2+} entry through the Na^+-Ca^{2+} exchanger as trigger for Ca^{2+} release from the sarcoplasmic reticulum. A comparison between L-type Ca^{2+} current and reverse-mode Na^+-Ca^{2+} exchange. *Circ Res* 81: 1034–1044, 1997.
32. **Somers VK, White DP, Amin R, Abraham WT, Costa F, Culebras A, Daniels S, Floras JS, Hunt CE, Olson LJ, Pickering TG, Russell R, Woo M, Young T.** Sleep apnea and cardiovascular disease. An American Heart Association/American College of Cardiology Foundation Scientific Statement From the American Heart Association Council for High Blood Pressure Research Professional Education Committee, Council on Clinical Cardiology, Stroke Council, and Council on Cardiovascular Nursing Council. *Circulation* 118: 1080–111, 2008.
33. **Tahawi Z, Orolinova N, Joshua IG, Bader M, Fletcher EC.** Altered vascular reactivity in arterioles of chronic intermittent hypoxic rats. *J Appl Physiol* 90: 2007–2013, 2001.

34. **Tóth A, Kiss L, Varró A, Nánási PP.** Potential therapeutic effects of Na^+/Ca^{2+} exchanger inhibition in cardiac diseases. *Curr Med Chem* 16: 3294–3321, 2009.
35. **Williams AL, Chen L, Scharf SM.** Effects of allopurinol on cardiac function and oxidant stress in chronic intermittent hypoxia. *Sleep Breath* 14: 51–57, 2010.
36. **Young T, Palta M, Dempsey J, Skatrud J, Weber S, Badr S.** The occurrence of sleep-disordered breathing among middle-aged adults. *N Engl J Med* 328: 1230–1235, 1993.
37. **Zhang J, Ren C, Chen L, Navedo MF, Antos LK, Kinsey SP, Iwamoto T, Philipson KD, Kotlikoff MI, Santana LF, Wier WG, Matteson DR, Blaustein MP.** Knockout of Na^+/Ca^{2+} exchanger in smooth muscle attenuates vasoconstriction and L-type Ca^{2+} channel current and lowers blood pressure. *Am J Physiol Heart Circ Physiol* 298: H1472–H1483, 2010.
38. **Zulian A, Baryshnikov SG, Linde CI, Hamlyn JM, Ferrari P, Golovina VA.** Upregulation of Na^+/Ca^{2+} exchanger and TRPC6 contributes to abnormal Ca^{2+} homeostasis in arterial smooth muscle cells from Milan hypertensive rats. *Am J Physiol Heart Circ Physiol* 299: H624–H633, 2010.